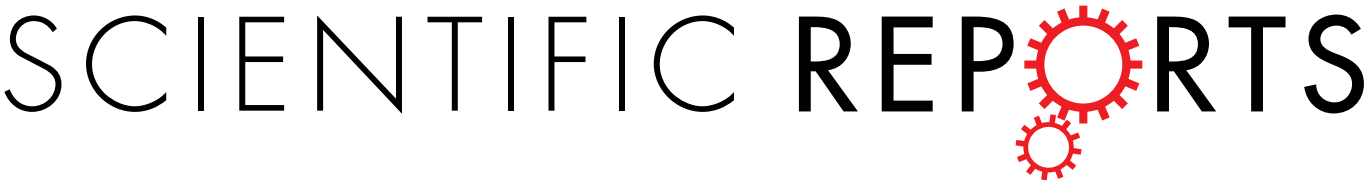

OPEN

Metabolic and diffusional limitations of photosynthesis in fluctuating irradiance in *Arabidopsis thaliana*

Received: 05 May 2016
Accepted: 11 July 2016
Published: 09 August 2016

Elias Kaiser[1,*,†], Alejandro Morales[2,*], Jeremy Harbinson[1], Ep Heuvelink[1], Aina E. Prinzenberg[1,3] & Leo F. M. Marcelis[1]

A better understanding of the metabolic and diffusional limitations of photosynthesis in fluctuating irradiance can help identify targets for improving crop yields. We used different genotypes of *Arabidopsis thaliana* to characterise the importance of Rubisco activase (Rca), stomatal conductance (g_s), non-photochemical quenching of chlorophyll fluorescence (NPQ) and sucrose phosphate synthase (SPS) on photosynthesis in fluctuating irradiance. Leaf gas exchange and chlorophyll fluorescence were measured in leaves exposed to stepwise increases and decreases in irradiance. *rwt43*, which has a constitutively active Rubisco enzyme in different irradiance intensities (except in darkness), showed faster increases than the wildtype, Colombia-0, in photosynthesis rates after step increases in irradiance. *rca-2*, having decreased Rca concentration, showed lower rates of increase. In *aba2-1*, high g_s increased the rate of change after stepwise irradiance increases, while in C24, low g_s tended to decrease it. Differences in rates of change between Colombia-0 and plants with low levels of NPQ (*npq1-2*, *npq4-1*) or SPS (*spsa1*) were negligible. In Colombia-0, the regulation of Rubisco activation and of g_s were therefore limiting for photosynthesis in fluctuating irradiance, while levels of NPQ or SPS were not. This suggests Rca and g_s as targets for improvement of photosynthesis of plants in fluctuating irradiance.

In physiological research, plants are often studied under constant environmental conditions. However, plants grow in a variable environment, with changes occurring in the time range of seconds or less[1]. Of the factors important for net photosynthesis (A_n), irradiance changes most quickly[2], causing a lag between changes in irradiance and changes in A_n, due to the slower regulation of photosynthesis[3]. This lag decreases light-use efficiency relative to the steady state and transiently increases excess irradiance, possibly harming the photosynthetic apparatus[4]. Leaves engage various mechanisms in response to fluctuating irradiance. Among the best known mechanisms are the regulation of enzymes of carbon fixation and sucrose metabolism, non-photochemical energy dissipation and stomatal conductance (g_s[3,5]). Although difficult to measure, cyclic electron transport may be another important mechanism (recently reviewed by Yamori and Shikanai[6]), due to a potential regulatory role and the balance of ATP versus NADPH production. During induction of photosynthesis in leaves adapted to darkness or low irradiance, the slow regeneration of ribulose-1,5-bisphosphate (RuBP) is typically most limiting until 60 seconds after illumination[7]. Thereafter, both the slow carboxylation due to partially inactive Rubisco (time to full activation: ~10 minutes) and slow stomatal opening (10–60 minutes) can limit the rate at which photosynthesis increases[8]. Thus, the slow rate of change of these mechanisms results in the lag between changes in irradiance and A_n and the resulting reduction of plant productivity[9]. Reductions in assimilation due to these physiological limitations can be up to 35% per day (subject to light environment and genotype[10]), and understanding them better may pave the road towards higher yields[11,12].

[1]Horticulture and Product Physiology Group, Department of Plant Sciences, Wageningen University, PO Box 16, 6700 AA Wageningen, The Netherlands. [2]Centre for Crop Systems Analysis, Department of Plant Sciences, Wageningen University, PO Box 430, 6700 AK Wageningen, The Netherlands. [3]Laboratory of Genetics, Department of Plant Sciences, Wageningen University, PO Box 16, 6700 AA Wageningen, The Netherlands. [†]Present address: Wageningen UR Greenhouse Horticulture, 6700 AP Wageningen, The Netherlands. [*]These authors contributed equally to this work. Correspondence and requests for materials should be addressed to E.K. (email: elias.kaiser@wur.nl)

Our understanding of the metabolic constraints of photosynthesis in fluctuating irradiance (hereafter: 'dynamic photosynthesis') have mainly come from biochemical studies[7,13,14], with less use being made of genetic diversity. Naturally occurring ecotypes, mutations, cultivars and genetically modified accessions offer a range of genotypes with specific properties, that could be used to study dynamic photosynthesis[5]. *Arabidopsis thaliana* possesses a wide, well documented genotypic diversity, which has been extended by selecting for mutations and by transgenic modifications.

Rubisco catalyses CO_2 assimilation and its activation limits A_n after irradiance increases[13,15]. In the chloroplast stroma, several inhibitory compounds are present and bind to Rubisco. To maintain sufficient Rubisco activity, these inhibitors must be removed from the active sites by the ATPase Rubisco activase (Rca[16]). In *Arabidopsis thaliana*, there are two isoforms of Rca, the larger α-isoform and the smaller β-isoform[17]. In plants containing both isoforms, redox-regulation of the α-isoform affects the ADP sensitivity of the holoenzyme (composed of both isoforms[18,19]). In low irradiance (i.e. high ADP/ATP ratio), the α-isoform is less active and the rate of overall Rubisco activation is low. Since Rca is a central regulator of Rubisco activity, how these isoforms, or their concentration affect dynamic photosynthesis is an important yet unresolved question.

After CO_2 assimilation by Rubisco, a fraction of the triose phosphates leaves the chloroplast in exchange for orthophosphate (P_i) from the cytosol. In the cytosol, triose phosphate is converted to sucrose, and sucrose phosphate synthase (SPS) plays a central role in this pathway[20]. In certain circumstances, such as photosynthetic induction in saturating CO_2, irradiance-dependent activation of SPS can be slower than that of Calvin cycle enzymes, making the Calvin cycle transiently P_i-limited[14]. Furthermore, after irradiance decreases, an overshoot in sucrose synthesis can transiently drain metabolites from the Calvin cycle, transiently decreasing A_n[21]. Plants with reduced SPS concentration may therefore exhibit slower increases in A_n after irradiance increases, and a smaller transient dip in A_n after irradiance decreases.

Leaves protect themselves from absorbed irradiance that is in excess of the capacity of photochemistry using non-photochemical quenching (NPQ). This protection, however, may come at a price. Sustained high levels of NPQ after irradiance decreases may result in transient limitations of the quantum efficiency of photosystem II for electron transport (ϕ_{PSII}). Model calculations indicate that slow relaxation of NPQ could decrease canopy photosynthesis by ~13–24%[22]. NPQ has been shown to limit A_n in genotypes with faster NPQ buildup after irradiance increases[23] or slower NPQ relaxation after irradiance decreases[24]. Thus, genotypes with constitutively low NPQ may have increased dynamic photosynthesis rates, principally as a result of less limitation on A_n following a decrease in irradiance.

In many plants, stomata open when irradiance increases. Typically, stomatal opening is slow, transiently limiting A_n during the irradiance increase[25]. Genotypes with constitutively high g_s may not experience this limitation[26], and may therefore be more productive in environments with a high proportion of fluctuating irradiance, provided that water is not limiting.

We used several genotypes, i.e. plants containing point mutations, transformants, T-DNA insertion lines (SALK lines[27]) and naturally occurring accessions of *A. thaliana*, to analyse how metabolic (Rubisco activation, sucrose synthesis, NPQ) and diffusional (g_s) limitations affect dynamic photosynthesis. In addition to measuring their steady-state photosynthetic irradiance and CO_2 responses, we exposed these genotypes to stepwise increases and decreases in irradiance, while measuring gas exchange and chlorophyll fluorescence. To investigate the effects of Rca regulatory properties or concentrations, we used the transformant *rwt43* (lacks the α-isoform of Rca and is therefore ADP-insensitive[19]) and the mutant *rca-2*, which is due to a leaky allele mutation (decreased Rca concentration[28]). To analyze the effect of SPS, we studied the T-DNA mutant line *spsa1* (80% reduction in maximum SPS activity[29]). The effect of low NPQ was investigated by using *npq4-1* (lacks PsbS, greatly diminishing NPQ[30]) and *npq1-2* (lacks zeaxanthin deepoxidase and therefore violaxanthin, diminishing NPQ[31]). Effects of high and low g_s were analyzed by using *aba2-1* (impaired abscisic acid (ABA) synthesis, leading to constitutively high g_s[32]) and the natural accession C24 (low g_s[33]), respectively. The accession Col-0 is the wildtype background to all mutants and transformants used in this study and acts as a control line. This study indicates that wildtype isoform composition and amount of Rca, as well as g_s limit dynamic photosynthesis in *A. thaliana*, while wildtype levels of SPS and NPQ do not.

Results

Steady-state responses to irradiance and CO_2 confirm genotypic effects on Rubisco activation state, sugar metabolism and stomatal conductance. To characterize the steady-state behaviour of the different *A. thaliana* genotypes we measured their responses to irradiance and leaf internal CO_2 concentration (C_i). Rates of A_n in Col-0 were comparable to studies using plants grown under similar conditions[34–37]. In the mutant containing less Rca, *rca-2*, irradiance-saturated A_n was lower than for Col-0, and saturation occurred around 600 μmol m^{-2} s^{-1} (Fig. 1a). The lower C_i response on A_n in *rca-2* (Fig. 1b) resulted in significantly decreased maximum carboxylation rate by Rubisco (V_{cmax}; −23%), maximum rate of electron transport (J_{max}; −14%) and maximum rate of triose phosphate utilisation (TPU; −7%) compared to Col-0 (Table 1). Assimilation in the transformant lacking the α-isoform of Rca, *rwt43*, exhibited similar irradiance and C_i responses as in Col-0 (Fig. 1). In the mutant with less SPS (*spsa1*), A_n did not differ from Col-0 in its irradiance response (Fig. 1a), but was strongly reduced at high C_i (Fig. 1b), resulting in decreased J_{max} (−14%) and TPU (−23%). The ABA-deficient mutant, *aba2-1,* showed larger irradiance- and CO_2-saturated photosynthesis rates compared to Col-0, while the accession C24 showed the opposite (Fig. 1c,d). Some parameters derived from C_i response curves were therefore larger in *aba2-1* (J_{max}: +18%, TPU: +19%), while they were smaller in C24 (V_{cmax}: −17%, J_{max}: −20%, TPU: −22%). The supply lines[38] (Fig. 1d) emphasize differences in g_s between C24, Col-0 and *aba2-1*: the steeper the slope, the smaller the difference between external CO_2 concentration (C_a) and C_i, and the larger g_s. Irradiance and C_i responses of photosynthesis of low-NPQ mutants (*npq1-2*, *npq4-1*) were similar to Col-0 (Fig. 1e,f), except for lower J_{max} in *npq4-1* (−7%). The response of quantum yield of photosystem II (ϕ_{PSII}) to C_i largely paralleled

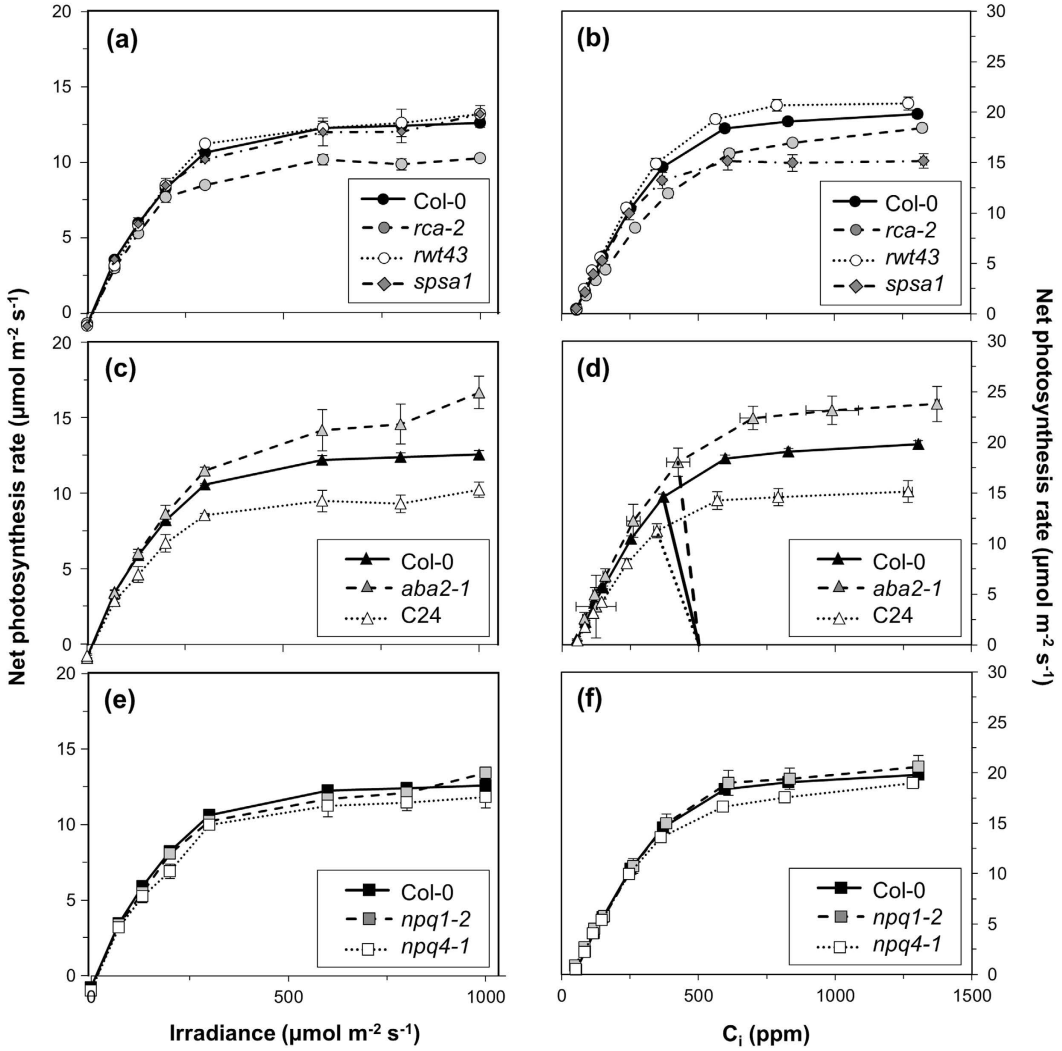

Figure 1. Irradiance and CO_2 response of net photosynthesis rates in *rca-2*, *rwt43* and *spsa1* (**a,b**), *aba2-1* and C24 (**c,d**) and *npq1-2* and *npq4-1* (**e,f**). Col-0 is included in each panel for ease of comparison. In (**d**), supply lines[38] between $C_a = 500$ and the corresponding C_i response curve of A_n are shown to emphasize stomatal effects of *aba2-1*, C24 and Col-0 on C_i. Averages ± SEM, n = 5–15.

	V_{cmax}	J_{max}	TPU	RMSE
Col-0	53 ± 1	100 ± 2	7.1 ± 0.1	0.93 ± 0.04
rca-2	40 ± 1***	86 ± 2***	6.7 ± 0.1 n.s.	0.95 ± 0.11 n.s.
rwt43	57 ± 3 n.s.	105 ± 5 n.s.	7.5 ± 0.2 n.s.	0.98 ± 0.07 n.s.
spsa1	54 ± 4 n.s.	86 ± 5**	5.5 ± 0.3***	0.85 ± 0.06 n.s.
aba2-1	58 ± 3 n.s.	118 ± 6***	8.5 ± 0.6**	1.12 ± 0.11 n.s.
C24	44 ± 2**	79 ± 4***	5.5 ± 0.4***	0.76 ± 0.07*
npq1-2	52 ± 3 n.s.	101 ± 5 n.s.	7.4 ± 0.4 n.s.	0.95 ± 0.08 n.s.
npq4-1	53 ± 1 n.s.	92 ± 2*	6.8 ± 0.2 n.s.	0.98 ± 0.03 n.s.

Table 1. Parameters derived from C_i response curves of A_n. V_{cmax}, maximum caboxylation rate by Rubisco (µmol CO_2 m^{-2} s^{-1}); J_{max}, maximum rate of electron transport in the absence of regulation (µmol electrons m^{-2} s^{-1}); TPU, maximum rate of triose phosphate utilisation (µmol CO_2 m^{-2} s^{-1}). The root mean squared error (RMSE, µmol CO_2 m^{-2} s^{-1}) of the differences between measurement and model during curve fitting[55] is shown as an estimation of the overall goodness of fit. Averages ± SEM, n = 5–15. Stars within columns denote significance levels compared to Col-0: ***$P < 0.0001$, **$P < 0.01$, *$P < 0.05$. Absence of stars denotes lack of significant difference with Col-0 ($P > 0.05$).

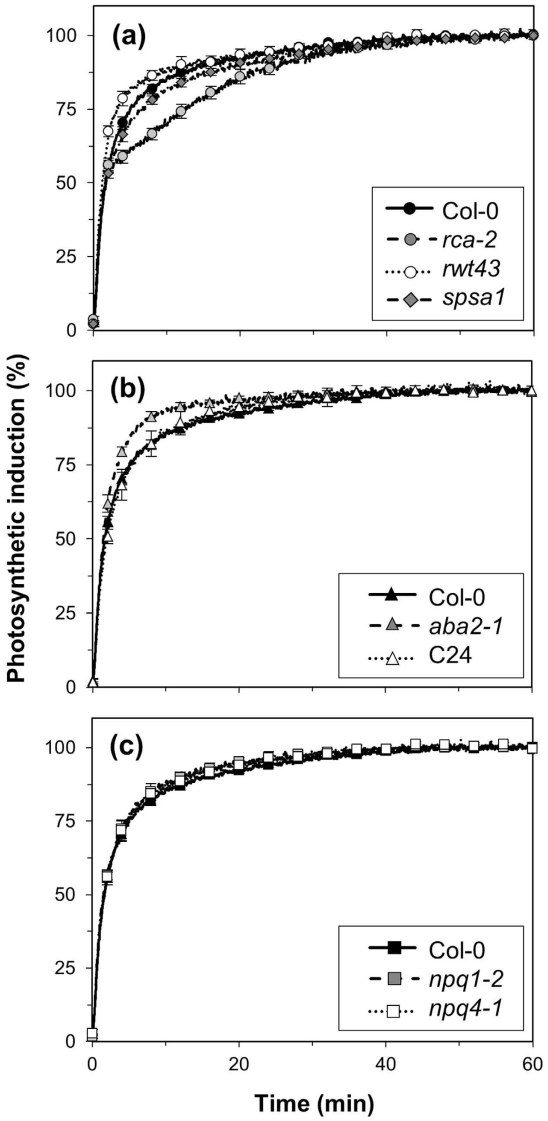

Figure 2. Photosynthetic induction after a step increase in irradiance from 0 to 1000 μmol m^{-2} s^{-1} in *rca-2, rwt43* and *spsa1* (**a**), *aba2-1* and C24 (**b**) and *npq1-2* and *npq4-1* (**c**). Col-0 is included in each panel for ease of comparison. Averages ± SEM, n = 5–15.

that of A_n, with the exception that ϕ_{PSII} decreased at high C_i in many genotypes (except *rca-2* and *npq4-1*; see Supplementary Fig. 1). This decrease in ϕ_{PSII} was most marked, and started at a lower C_i, in *spsa1* (Supplementary Fig. 1a).

Larger Rubisco activation state and g_s accelerate photosynthetic induction, while lower NPQ does not. Next, we characterised the dynamic behaviour of leaf gas exchange by inducing photosynthesis in dark-adapted leaves using a stepwise increase to saturating irradiance (1000 μmol m^{-2} s^{-1}). Rates of photosynthetic induction were initially similar between all genotypes (except *rwt43*) until ~60% induction was reached (Fig. 2). *rwt43* reached 50% of photosynthetic induction (t_{A50}) significantly faster than Col-0 (Table 2). Induction remained faster in *rwt43* until it reached ~80% (Fig. 2a). In *rca-2*, the rate of induction slowed after 60% completion and then increased in a nearly linear fashion rather than the more exponential increase shown by all other genotypes (Fig. 2a). This increased the time to reach 90% of photosynthetic induction (t_{A90}) by ~10 minutes compared to Col-0. *spsa1* showed slightly slower induction rates (Fig. 2a), increasing t_{A90} by ~5 min compared to Col-0. *aba2-1* exhibited faster induction, halving the t_{A90} of Col-0, while induction in C24 was identical to that of Col-0 (Fig. 2b). Induction in *npq1-2* and *npq4-1* was identical to Col-0 (Fig. 2c).

To explain the differences between genotypes affecting Rubisco activation and g_s, we looked at the time courses of C_i, diffusional limitation and biochemical limitation. While C_i in Col-0 and *rwt43* dropped by ~130 ppm within 10 minutes and then increased by 30–40 ppm following stomatal opening, in *rca-2* it never dropped below its final value (Fig. 3a). Diffusional limitation reached its maximum within ~10 minutes in Col-0 and *rwt43* and then relaxed, while in *rca-2* its increase was much slower and levelled off after ~30 minutes (Fig. 3c). Biochemical

Genotype	$0 \rightarrow 1000\,\mu mol\,m^{-2}\,s^{-1}$		$70 \rightarrow 800\,\mu mol\,m^{-2}\,s^{-1}$		$130 \rightarrow 600\,\mu mol\,m^{-2}\,s^{-1}$	
	t_{A50}	t_{A90}	t_{A50}	t_{A90}	t_{A50}	t_{A90}
Col-0	1.6 ± 0.1	14.7 ± 1.2	1.3 ± 0.1	10.2 ± 1.1	0.6 ± 0.0	9.0 ± 2.2
rca-2	1.5 ± 0.2	25.5 ± 1.5***	6.3 ± 0.4***	30.9 ± 2.0***	4.0 ± 0.7***	29.8 ± 1.7***
rwt43	1.2 ± 0.1**	14.2 ± 2.6	0.5 ± 0.0***	16.2 ± 6.1	0.3 ± 0.0***	18.8 ± 6.1
spsa1	1.6 ± 0.1	19.5 ± 1.3*	1.3 ± 0.1	14.1 ± 7.2	0.6 ± 0.1	13.7 ± 6.9
aba2-1	1.4 ± 0.1	7.3 ± 0.5**	1.3 ± 0.1	7.7 ± 2.6	0.8 ± 0.1	15.1 ± 5.8
C24	1.9 ± 0.1	15.0 ± 3.2	1.7 ± 0.3*	13.3 ± 2.7	0.9 ± 0.2*	29.4 ± 5.1***
npq1-2	1.4 ± 0.1	11.7 ± 1.7	1.3 ± 0.1	10.7 ± 2.9	0.7 ± 0.0	14.6 ± 8.6
npq4-1	1.5 ± 0.1	14.8 ± 2.6	1.1 ± 0.1	6.1 ± 0.7	0.6 ± 0.0	15.3 ± 11.0

Table 2. Time (minutes) to reach 50 and 90% of steady-state photosynthesis rates (t_{A50}, t_{A90}) after step increases in irradiance. Averages ± SEM, n = 5–15. Stars within columns denote significance levels compared to Col-0: ***$P < 0.0001$, **$P < 0.01$, *$P < 0.05$. Absence of stars denotes lack of significant difference with Col-0 ($P > 0.05$).

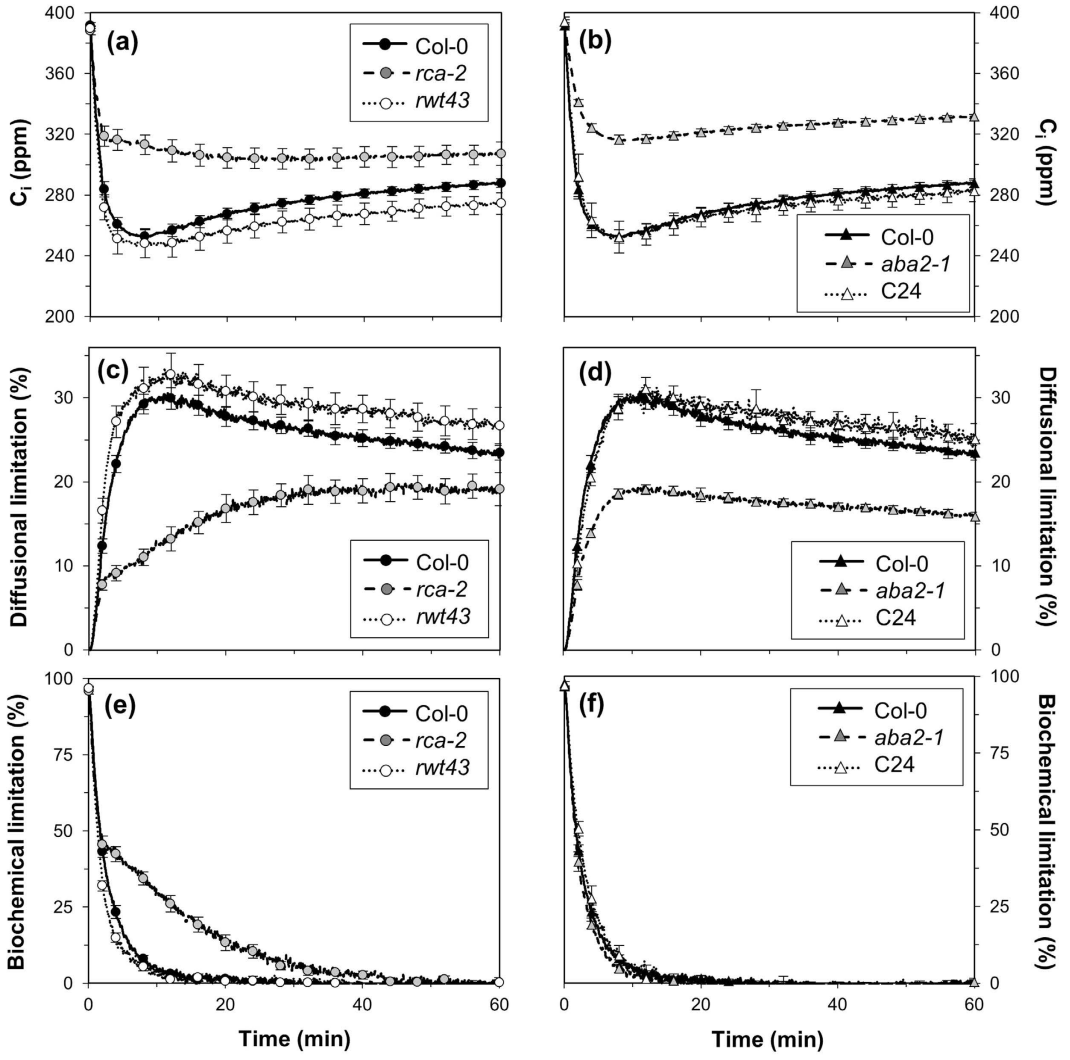

Figure 3. Leaf internal CO_2 concentration (C_i), diffusional limitation and biochemical limitation after a step increase in irradiance from 0 to 1000 μmol m^{-2} s^{-1} in Col-0, *rca-2* and *rwt43* (**a**,**c**,**e**) and Col-0, *aba2-1* and C24 (**b**,**d**,**f**). Averages ± SEM, n = 5–15.

limitation during induction relaxed almost completely within ~10 minutes in Col-0 and *rwt43*, while in *rca-2* it was generally greater and the same extent of relaxation took ~40 minutes (Fig. 3e). Comparing Col-0 and C24, the responses of C_i were almost indistinguishable, while in *aba2-1* the initial decrease in C_i was smaller, ranging from

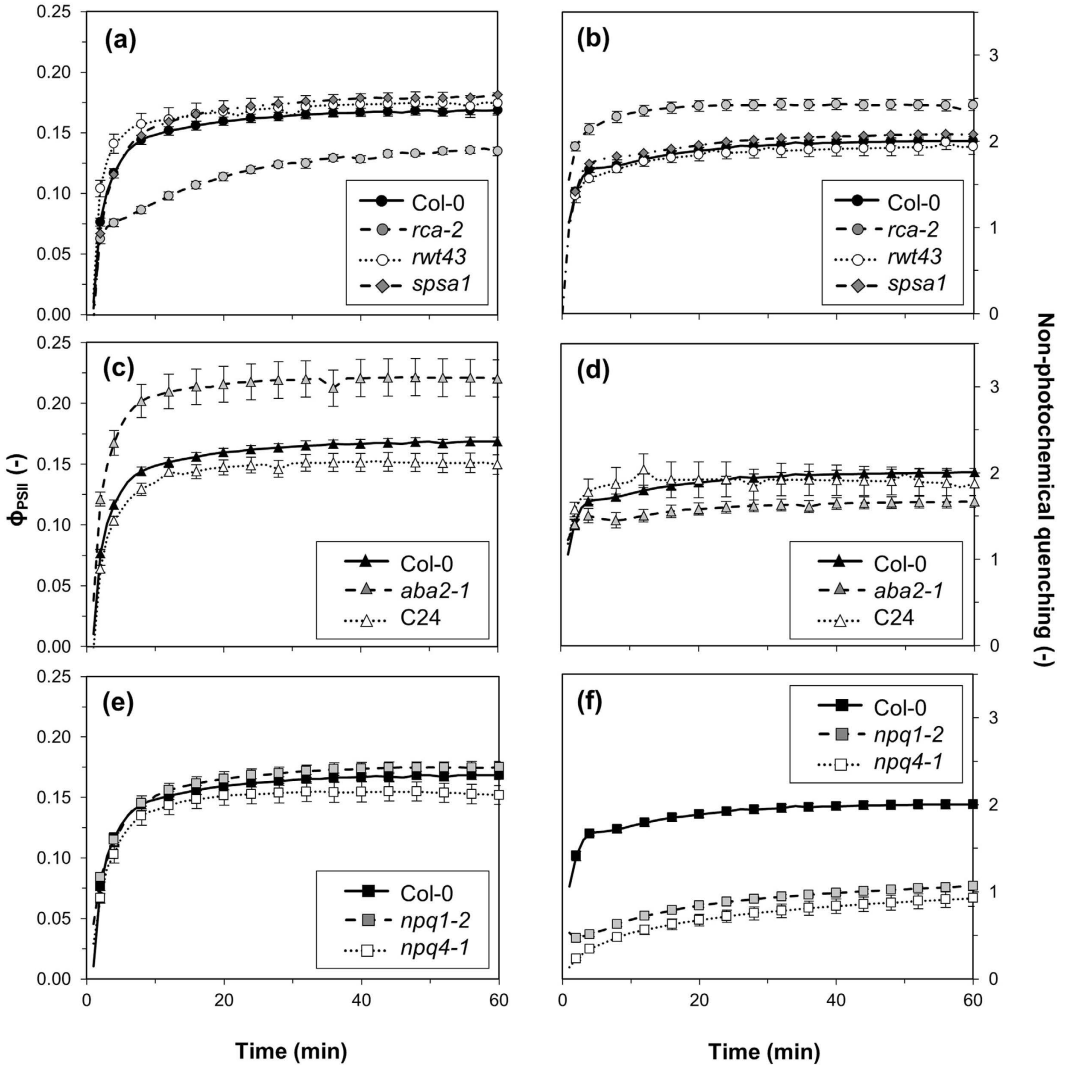

Figure 4. Quantum yield of photosystem II (ϕ_{PSII}) and non-photochemical quenching (NPQ) after a step increase in irradiance from 0 to 1000 μmol m^{-2} s^{-1} in *rca-2, rwt43* and *spsa1* (**a**,**b**), *aba2-1* and C24 (**c**,**d**) and *npq1-2* and *npq4-1* (**e**,**f**). Col-0 is included in each panel for ease of comparison. Averages ± SEM, n = 5–15.

50–60% of that found in Col-0 (Fig. 3b). Buildup and relaxation of diffusional limitation were much smaller in *aba2-1* (Fig. 3d), while relaxation of biochemical limitation was similar between Col-0, *aba2-1* and C24 (Fig. 3f).

Next to the dark-light transition discussed above, we also exposed leaves that had been adapted to low irradiance (hereafter: background irradiance) to stepwise increases in irradiance, namely 70 → 800 and 130 → 600 μmol m^{-2} s^{-1}. The responses of A_n to these increases were qualitatively similar to those seen after the dark-light transition (Supplementary Fig. 2). *rwt43* exhibited a faster increase, and *rca-2* a much slower increase than Col-0 (Supplementary Fig. 2a,b). This reduced t_{A50}, but not t_{A90}, in *rwt43*, while t_{A50} and t_{A90} in *rca-2* were larger than Col-0 (Table 2). C24 tended to increase photosynthesis more slowly compared to Col-0 (Supplementary Fig. 2c,d), leading to a larger t_{A50} after the 70 → 800 μmol m^{-2} s^{-1} step increase and larger t_{A50} and t_{A90} after the 130 → 600 μmol m^{-2} s^{-1} step increase. Assimilation responses in NPQ and SPS mutants to those intermediate irradiance increases were similar to Col-0.

Apart from gas exchange dynamics, we also characterised changes in electron transport parameters after the stepwise 0–1000 μmol m^{-2} s^{-1} transition. Changes in ϕ_{PSII} largely paralleled those of A_n (Fig. 4). In *rwt43*, the increase in ϕ_{PSII} was slightly faster than in Col-0, while in *rca-2*, it was slower and steady-state ϕ_{PSII} was lower (Fig. 4a), paralleling its lower steady-state A_n (Fig 1a). Despite slightly larger ϕ_{PSII} throughout induction in *spsa1*, final values were not significantly different from Col-0 (P = 0.09, Fig. 4a). *aba2-1* showed increased steady-state ϕ_{PSII} levels, while in C24 they were reduced compared to Col-0 (Fig. 4c), similar to the differences in steady-state assimilation (Fig. 1c). In *npq4-1*, ϕ_{PSII} was slightly lower during induction than in *npq1-2* and Col-0 (*npq1-2* had similar ϕ_{PSII} trends and values during induction as Col-0; Fig. 4e). NPQ in *rca-2* increased more quickly to its steady-state level, which was larger than that of Col-0, *spsa1* and *rwt43* (Fig. 4b). NPQ in *aba2-1* was lower than in Col-0 and C24 (which were not significantly different from each other, Fig. 4d). As expected, *npq1-2* and *npq4-1* developed much lower NPQ levels than Col-0, and NPQ buildup was slower compared to Col-0, but similar in

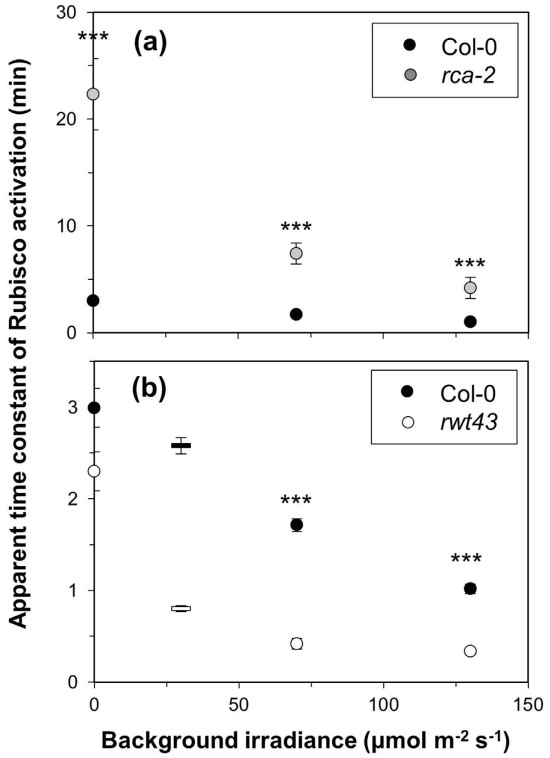

Figure 5. Apparent time constant of Rubisco activation in *rca-2* (**a**) and *rwt43* (**b**), compared to Col-0. Note the different scales of Y-axes in (**a**,**b**). Averages ± SEM, n = 5–15. Bars in (**b**) at 30 μmol m^{-2} s^{-1} background irradiance included from Carmo-Silva and Salvucci[42]. Stars denote significance levels of single genotypes compared to Col-0: ***$P < 0.001$.

both *npq1-2* and *npq4-1* (Fig. 4f). Dark-adapted F_v/F_m was 0.805 ± 0.002 (Avg ± standard error of the mean, SEM) in Col-0. In *rca-2*, C24 and *npq4-1*, F_v/F_m was marginally, but significantly, smaller, possibly due to photoinhibition that was not completely removed by dark adaptation. In *spsa1*, it was slightly but significantly higher than in Col-0 (Supplementary Fig. 3).

Isoform, amount and initial activation state of Rca affect the rate of Rubisco activation. The apparent time constants of Rubisco activation (τ_R, the time to reach 63% of total change in Rubisco activation state), decreased with increasing background irradiance (Fig. 5). Genotypes differing in g_s, NPQ and SPS did not differ from Col-0 in τ_R. However, τ_R tended to be 17–28% larger in *spsa1* than in Col-0; *P*-values ranged from 0.07 to 0.09. Of the genotypes affecting Rca regulation, *rca-2* exhibited the biggest differences in τ_R, both compared with Col-0 ($P < 0.001$ in all cases) and between background irradiances, with a τ_R of ~22 minutes in dark-adapted leaves decreasing to ~4 minutes in leaves adapted to an irradiance of 130 μmol m^{-2} s^{-1} (Fig. 5a). In *rwt43*, τ_R of dark-adapted leaves (2.3 min) was not significantly different to that of Col-0 (3.0 min; $P = 0.08$), but was significantly ($P < 0.001$) smaller at 70 and 130 μmol $m^{-2}s^{-1}$ background irradiance (Fig. 5b).

Increases in initial g_s up to a threshold value accelerate photosynthetic induction. Before and after stepwise increases in irradiance, g_s was considerably higher in *aba2-1* than in Col-0 and C24 (Supplementary Fig. 4). In dark-adapted leaves of Col-0 and C24, g_s was similar, but in leaves adapted to 70 or 130 μmol m^{-2} s^{-1}, it was almost twice as high in Col-0 compared to C24. This spread in g_s was used to explore the threshold between a limiting and a non-limiting initial g_s for the subsequent rates of A_n increase. For example, after the 0 → 1000 μmol m^{-2} s^{-1} increase, t_{A90} was lower in plants with initially higher g_s up to ~0.13 mol m^{-2} s^{-1}, but above 0.13 mol m^{-2} s^{-1} there was no further decrease in t_{A90} (Fig. 6). This shows that an initial $g_s > 0.13$ mol m^{-2} s^{-1} was non-limiting in this case. We also looked at various time points (t_{A10}, t_{A20}, etc.) after different low-to-high irradiance transitions (i.e. 0 → 1000, 70 → 800 and 130 → 600 μmol m^{-2} s^{-1}) and found that the threshold between limiting and non-limiting initial g_s was between 0.09 and 0.17 mol m^{-2} s^{-1}, with no discernible trend between time points or background irradiance levels.

Apart from the effect of initial g_s on the rate of A_n increase, we also analysed the effects of g_s increase after stepwise increases in irradiance (Supplementary Fig. 4). In C24 and Col-0, the increase in g_s after the 0 → 1000 μmol m^{-2} s^{-1} increase (until 60 minutes after the start of illumination) and t_{A90} correlated positively (Supplementary Fig. 5). Because initial g_s in *aba2-1* was high, it was non-limiting to rates of increase in photosynthesis after irradiance increases, and stomatal opening did not correlate with t_{A90} (data not shown).

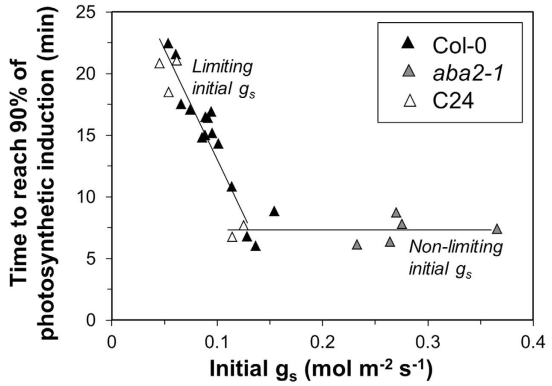

Figure 6. Relationship between initial g_s and the time to reach 90% of final photosynthesis rates after a step increase in irradiance (0–1000 μmol m^{-2} s^{-1}) in single replicates of Col-0, *aba2-1* and C24.

Lower NPQ and SPS do not increase transient photosynthesis after a decrease in irradiance.

After step decreases in irradiance (600 → 200, 800 → 130 μmol m^{-2} s^{-1}), relative changes in A_n were similar for all genotypes (Supplementary Fig. 6), and there were no significant differences in either post-illumination CO_2 fixation or the post-illumination CO_2 burst, including the NPQ mutants and *spsa1* (Supplementary Fig. 7).

Discussion

Making use of the genetic diversity available for *A. thaliana*, we explored several possible physiological limitations of dynamic photosynthesis. This analysis revealed that altered Rubisco activation kinetics or stomatal conductance affect photosynthesis in a dynamic irradiance environment greatly, while alterations in non-photochemical quenching or sucrose synthesis do not.

Changes affecting Rca concentration (*rca-2*) or regulation (*rwt43*) had strong effects on dynamic photosynthesis. The observed effects were likely caused by different kinetics of Rubisco activation, as the initial increase in assimilation after dark-light transitions (first minute in Fig. 2a) was similar between genotypes, implying a similar limitation due to activation of RuBP regeneration (Sassenrath-Cole and Pearcy[7] provided biochemical evidence for this). Furthermore, these genotypes had similar g_s (Supplementary Fig. 8). Lower steady-state irradiance and CO_2 responses in *rca-2* may have been caused by a reduced steady-state activation of Rubisco[39]. Based on the dependency between maximum Rubisco activation state and Rca concentration reported by Mott and Woodrow[40] and our estimation of V_{cmax} for *rca-2* (Table 1), we estimate that *rca-2* contains ~22% of wildtype Rca levels (Supplementary text 1). The effects on the rate of Rubisco activation of such low Rca content are apparent. In antisense or overexpressors of Rca in rice, a positive linear relationship between Rca concentration and the rate of photosynthetic induction was shown for various temperatures[41], demonstrating the role of Rca concentration in controlling dynamic photosynthesis. Intriguingly, in our study τ_R decreased with background irradiance (Fig. 5). While this decrease was linear in Col-0, it resembled a negative exponential in *rwt43*. This is in agreement with data of Carmo-Silva and Salvucci[42] (Fig. 5b). Previous studies have shown that Rubisco activation in Col-0 increased linearly with irradiance[42–44], while in *rwt43*, Rubisco activation state did not change with increasing irradiance[42]; it was similar to Col-0 in dark-adapted leaves, but close to full activation in low irradiance[19,42,44]. Most likely differences in the activation state of Rca, rather than that of Rubisco, caused τ_R to decrease with background irradiance. Rca activity increased linearly between 0 and 300 μmol m^{-2} s^{-1} in intact spinach leaves[45], and should be high in *rwt43* except in darkness (see above).

Compared to natural fluctuations in irradiance, stomata open and close slowly[46]. Low initial g_s can become a limitation to carbon fixation after a step change in irradiance[2], because of comparably rapid activation of RuBP regeneration and Rubisco. The peak of this limitation is typically reached within ~10 minutes due to Rubisco activation without similarly large increases in g_s, after which it relaxes due to stomatal opening (Fig. 3d). We note that the index of diffusional limitation should be refined with respect to changes in Rubisco activation during photosynthetic induction, as well as possible changes in mesophyll conductance (g_m) during transients. With respect to g_m, contrasting responses to irradiance have been reported (cf. refs 47 and 48); we therefore refrain from speculations on how it may have changed in our measurements but note that it may have affected the index of diffusional limitation. Nevertheless, we believe that diffusional limitation provides a useful qualitative tool to analyse the differences between the genotypes affecting Rubisco activation kinetics and g_s.

The mutant with high initial g_s (*aba2-1*) did not show such large differences in stomatal opening (i.e. difference between initial and final g_s; Supplementary Fig. 4), but still had much higher rates of A_n increases when irradiance was raised. Therefore, we argue that increasing the initial g_s is a simpler route to increasing dynamic photosynthesis than is increasing the rate of stomatal opening. Stomatal closure in low irradiance is an adaptive response to changing water supply and logical under non-irrigated field conditions, however for crops in well-watered situations, increasing g_s at the expense of water use may be a reasonable target to increase rates of dynamic photosynthesis. Also, the threshold between limiting and non-limiting g_s for rates of photosynthesis increase could be used as a phenotypic marker for breeding of cultivars with non-limiting g_s in fluctuating irradiance. In our analysis, this threshold proved to be consistent, independent of the time point after stepwise increases in irradiance and level of background irradiance. Previous findings indicate that this threshold shows no diurnal variation[26],

and that it is unchanged by water stress[26] or growth light conditions[49]. An open question that remains is whether the threshold is species-specific[26] or not[49]. It is likely that a high initial g_s correlates with constitutively high g_s (i.e. stomata are more open and less sensitive to changes in irradiance), and faster responses of A_n to an increasing irradiance could be reached at the expense of lower intrinsic water use efficiency. Rapid screening for high g_s could be achieved by thermal imaging[50].

In Col-0, rates of NPQ buildup after a dark-light transition were similar to those seen in previous studies[51,52], while mutants *npq1-2* (lacking violaxanthin de-epoxidase[31]) and *npq4-1* (lacking PsbS[30]) exhibited a much lower buildup of NPQ. However, they showed negligible differences in gas exchange to Col-0, neither in their steady-state responses to irradiance and CO_2 (Fig. 1e,f) nor in their responses to step increases in irradiance (Fig. 2c, Supplementary Fig. 2e,f). Similar to our findings, reduced PsbS content in transgenic rice plants strongly reduced NPQ but had limited effects on carbon gain during a 5-min induction period[23]. In contrast, overexpressors with 2–4 fold increases in PsbS showed ~15% lower A_n during induction, demonstrating that increased energy dissipation can have adverse effects on assimilation[23]. Antisense mutants with reduced thylakoid membrane K^+ flux capacities showed less rapid relaxation of NPQ after irradiance decreases, reducing electron transport and assimilation[24]. Our data revealed no differences between *npq1-2*, *npq4-1* and Col-0 with respect to post-illumination CO_2 fixation (Supplementary Fig. 7), and therefore show that unlike the rate of NPQ relaxation[22,24], an initially low level of NPQ does not increase carbon gain directly after decreases in irradiance.

Irradiance-dependent activation of SPS is genotype-specific, and *A. thaliana* belongs to a group of species with low light/dark modulation of the enzyme[53]. This suggests that in the wildtype, SPS activity does not limit photosynthetic induction–however, in a plant with strongly reduced SPS concentration it might. We tested this possibility in the T-DNA mutant *spsa1*, which has a 80% lower maximum SPS activity than Col-0[29]. Similar to our findings, Sun *et al.*[29] found no photosynthetic differences between *spsa1* and Col-0, except for a strong reduction in CO_2-saturated A_n (−23%). Importantly, the decrease in SPS hardly affected photosynthetic responses to fluctuating irradiance. The only significant difference was a longer time to reach 90% of full induction after dark-light transitions (Table 2). However, no such differences were observed in transitions from low to higher irradiance. *spsa1* would probably show decreased rates of dynamic photosynthesis in elevated CO_2 concentrations. Furthermore, it may be that the absence of a measurable effect of *spsa1* on the post-illumination CO_2 burst, which is partly affected by the rate of sucrose synthesis[21], was masked by the photorespiratory portion of the CO_2 burst, which is most pronounced in C_3 plants[5]. Also, reduced levels of SPS in species that exhibit strong light/dark modulation of SPS (e.g. barley, maize, spinach and sugarbeet[53]) would probably have a stronger negative effect on photosynthetic induction than shown here for *A. thaliana*.

The relationship between ϕ_{PSII} and C_i in C_3 photosynthesis contains three phases: When A_n is (a) limited by Rubisco, ϕ_{PSII} increases with C_i; when A_n is (b) limited by RuBP regeneration, ϕ_{PSII} is constant with increases in C_i and when A_n is (c) limited by TPU, ϕ_{PSII} decreases with increasing C_i[54,55]. Most genotypes in our study did not show the plateau in ϕ_{PSII} that would signify a phase of RuBP regeneration limitation, with *spsa1* showing an extreme form of that behaviour (Supplementary Fig. 1). This suggests that (a) TPU occurs at a lower C_i than visible from gas exchange, (b) different limitations occur simultaneously within different layers of the leaf, (c) changes in the rate of cyclic electron transport around photosystem I and/or strength of alternative electron sinks or (d) with increasing C_i during the phase of limitation by RuBP regeneration photosynthetic electron transport is sometimes restricted, and ϕ_{PSII} is reduced, due to the increased inhibition of starch synthesis following the inhibition of phosphoglucoisomerase by phosphoglycerate[56]. However, these results have to be interpreted with caution because the number of data points between the end of Rubisco limitation and the onset of TPU was limited and more data may lead to different conclusions.

In conclusion, in *A. thaliana*, the presence of the redox-regulated α-isoform of Rca in the wildtype, and wildtype levels of g_s, are limiting for dynamic photosynthesis. Furthermore, reductions in Rca strongly decrease (dynamic) photosynthesis. We also show that wildtype levels of NPQ and SPS are not limiting in *A. thaliana*. This suggests Rca and g_s as targets for improvement of photosynthesis in fluctuating irradiance.

Methods

Plant material. Seeds of *npq4-1*, *spsa1* (SALK_148643C) and *rca-2* (SALK_003204C) were obtained from NASC (University of Nottingham, Loughborough, UK[57]). C24 (CS76106) was obtained from the Arabidopsis Biological Resource Center (ABRC, Ohio State University, USA). Seeds of Col-0 and *aba2-1* were obtained from Corrie Hanhart (Wageningen University, the Netherlands), *npq1-2* was obtained from Dr. Shizue Matsubara (Forschungszentrum Jülich, Germany) and *rwt43* was obtained from Dr. Elizabete Carmo-Silva (Rothamsted Research, UK).

Growth conditions. Plants were grown in 0.37 L pots using soil with a 4:1 peat:perlite mixture. Pots were placed on irrigation mats, and mats were saturated daily to full capacity. Plants were fertilized weekly using a nutrient solution especially developed for Arabidopsis[58]. To inhibit algal growth, the soil was covered with black plastic film. Plants were grown in a growth chamber in short-day conditions (8 hours of light) to delay flowering[59] and thus ensure that leaves were large enough for gas-exchange measurements. Irradiance was 172 ± 4 μmol m^{-2} s^{-1} as supplied by LED lights (GreenPower LED production module deep red/white 120; Philips, Eindhoven, the Netherlands; Supplementary Fig. 9). Temperature was 23/18 °C (day/night) and relative humidity was 70%. Mutants lacking ABA (*aba2-1*) were sprayed with an aqueous solution containing 10 μmol mol^{-1} ABA (Sigma, St. Louis, U.S.A.) when plants were 2, 4 and 6 weeks old. This increases rosette growth compared to untreated *aba2-1* plants (data not shown). There was a period of 15 days between the last application of ABA and the first measurements on *aba2-1* plants.

Single genotypes were grown sequentially (approx. one batch per week). Five plants per batch were used for measurements. To monitor the quality of the growth system over time, Col-0 was grown in three batches, each

batch separated by several weeks. The number of replicates was therefore 15 for Col-0, and 5 for all other genotypes. The growth system produced very reproducible photosynthetic phenotypes of Col-0 (Supplementary Fig. 10).

Measurements. Measurements were performed using the LI-6400 portable photosynthesis system (Li-Cor Biosciences, Lincoln, Nebraska, USA) equipped with the leaf chamber fluorometer (Part No. 6400-40) on single leaves of plants that were 6–8 weeks old. Leaves large enough to cover the leaf chamber gasket (area: 2 cm^2, diameter: 1.6 cm) were used. Conditions in the cuvette were as follows: 23 °C air temperature, 70% relative humidity, 90/10% red/blue light mixture and 500 $\mu mol\ s^{-1}$ air flow rate. The choice of flow rate was a compromise between getting a fast time response of the measuring system (necessary in dynamic gas exchange studies), and the difference in CO_2 concentration between sample and reference air stream. Except for the CO_2-response curves, the external CO_2 mole fraction was kept at 400 ppm. The oxygen mole fraction was always 21%.

Stepwise increases in irradiance. Leaves were adapted to several background irradiances (0, 70 or 130 $\mu mol\ m^{-2}\ s^{-1}$) for 30–60 minutes (until A_n and g_s had visibly reached a steady state), and then exposed to single-step increases in irradiance, namely $0 \rightarrow 1000$, $70 \rightarrow 800$ and $130 \rightarrow 600\ \mu mol\ m^{-2}\ s^{-1}$. These intensities were chosen, after preliminary irradiance-response curves on Col-0 had shown that all but the highest (1000 $\mu mol\ m^{-2}\ s^{-1}$) intensity were in the sub-saturating range (Supplementary Fig. 11). Gas exchange was logged nominally every second. Logging was stopped when g_s reached a new steady state (this was assessed visually, and took a minimum of 30 minutes after the step increase), or 60 minutes after switching to 1000 $\mu mol\ m^{-2}\ s^{-1}$. Before and after the $0 \rightarrow 1000\ \mu mol\ m^{-2}\ s^{-1}$ increase, ϕ_{PSII} and NPQ were measured, using a measuring beam intensity of ~1 $\mu mol\ m^{-2}\ s^{-1}$ and a saturating pulse of ~7600 $\mu mol\ m^{-2}\ s^{-1}$ intensity and 1 s duration. In preliminary measurements on Col-0, the saturating pulse was sufficient to saturate F_m' in leaves adapted to 1000 $\mu mol\ m^{-2}\ s^{-1}$ (assessed following the manufacturer's recommendations for calibrating the saturating pulse: F_m' was not increased when using saturating pulses of intensity higher than 7600 $\mu mol\ m^{-2}\ s^{-1}$). The F_o and F_m relative fluorescence yields were measured in dark-adapted leaves. After the increase in irradiance, the F_m' relative fluorescence yield was measured every minute for the first ten minutes, and every two minutes thereafter. The regular application of saturating flashes transiently increased the leaf temperature by 0.4–0.7 °C across genotypes (temperature traces of Col-0 are representative of all genotypes, Supplementary Fig. 12). Also, our data (Kaiser *et al.*, unpublished) indicate that the regular application of saturating flashes of similar intensity and frequency in tomato (*Lycopersicon esculentum*) had no effects on leaf gas exchange during photosynthetic induction. The steady-state relative fluorescence yield, F_s, was measured continuously. Dark-adapted F_v/F_m, ϕ_{PSII} and NPQ were calculated as $F_v/F_m = (F_m - F_o)/F_m$, $\phi_{PSII} = (F_m' - F_s)/F_m'$ and $NPQ = (F_m - F_m')/F_m'$, respectively.

During transients, g_m and mitochondrial respiration (R_d) were assumed to be constant because, to our knowledge, changes in g_m and R_d have never been assessed for irradiance transients. R_d in the light was considered similar to genotype-specific steady-state respiration in the dark; this assumption is supported by measurements on several species[60]. For g_m, a value of 0.2 mol $m^{-2}\ s^{-1}$ was assumed for all genotypes, which is an average of three values determined on Col-0 of comparable photosynthetic capacity[35,61].

The time to reach 50 and 90% (i.e. t_{50} and t_{90}) of steady-state A_n was calculated for each irradiance increase. To increase robustness of these indices to experimental noise and outliers, time series were smoothed using a local polynomial regression[62] with a span of 5%. This means that, for each point in the time series, a polynomial of degree two was fitted using weighted least squares to a data window of size equal to 5% of the total size of the time series; the weight assigned to each point decreases with the distance from the central point.

Calculation of diffusional limitation, biochemical limitation and the apparent time constant of Rubisco activation. To calculate several parameters, A_n was corrected for transient changes in chloroplast CO_2 concentration (C_c). For diffusional limitation, A_n was multiplied by the relative rate by which A_n would increase if C_c during induction was equal to ambient CO_2 concentration, C_a ($A^*_{nC_a}$):

$$A^*_{nC_a} = A_n * \frac{f(C_a)}{f(C_c)} \tag{1}$$

Where $f(C_a)$ is the steady-state value of A_n at C_a (i.e. at 400 ppm), and $f(C_c)$ is the steady-state value of A_n at C_c. The relative effects of C_c on A_n were taken from steady-state A_n/C_c response curves by fitting local polynomial regressions (LOESS) in the range 50–500 ppm (Supplementary Fig. 13). Diffusional limitation was then determined as:

$$Diffusional\ limitation = \frac{A^*_{nC_a} - A_n}{A_{nC_a} - A_{ni}} \cdot 100 \tag{2}$$

Where A_{nCa} is the steady-state value of A_n at C_a and A_{ni} is the initial steady-state rate of A_n. Diffusional limitation is therefore a combination of possible limitations due to g_s and g_m during induction and in the steady state (i.e. it does not decrease to 0% at the end of the time course). For biochemical limitation and τ_R, A_n was multiplied ($A^*_{nC_a}$) by the relative rate by which A_n would increase if transient C_c was equal to final, steady-state C_c (C_{cf}), following Woodrow and Mott[15]:

$$A^*_{nC_c} = A_n * \frac{f(C_{cf})}{f(C_c)} \tag{3}$$

Where $f(C_{cf})$ is the solution for A_n at C_{cf}. Biochemical limitation was calculated after Allen and Pearcy[63]:

$$Biochemical\ limitation = \frac{A_{nf} - A^{*}_{nC_c}}{A_{nf} - A_{ni}} \cdot 100 \quad (4)$$

Throughout induction, biochemical limitation decreases from 100 to 0%, and therefore indicates the additional limitation imposed on A_n due to incomplete activation of several enzymes. Biochemical and diffusional limitations do not sum up to 100%, and are distinct. The apparent time constant of Rubisco activation (τ_R) was calculated after Woodrow and Mott[15]:

$$\tau_R = \frac{\Delta time}{\Delta\ \ln\ \cdot\ (A_{nf} - A^{*}_{nC_c})} \quad (5)$$

The range of timepoints ($\Delta time$) for calculating τ_R differed between background irradiances (Supplementary Fig. 14), and in some cases between genotypes. This was due to differences in the rate of change of photosynthesis, and included 120 data points in the case of $0 \rightarrow 1000\,\mu mol\ m^{-2}\ s^{-1}$ (all genotypes) and 40 (for *rwt43*) or 60 (all other genotypes) in the case of $70 \rightarrow 800$ and $130 \rightarrow 600\,\mu mol\ m^{-2}\ s^{-1}$. These ranges were selected by visual inspection. The average root mean squared error of the linear fits was $1.2\,\mu mol\ m^{-2}\ s^{-1}$ (range: 1.0–3.0 $\mu mol\ m^{-2}\ s^{-1}$).

Stepwise decreases in irradiance. Irradiance was decreased in the following steps: $800 \rightarrow 130$ and $600 \rightarrow 200\,\mu mol\ m^{-2}\ s^{-1}$. From the CO_2 exchange data, post-illumination CO_2 fixation[64] and post-illumination CO_2 bursts[65] were quantified. The former implies that photosynthesis is above the final steady-state value during the transient, while the latter implies a lower assimilation rate than at steady state. Values were estimated by integrating the difference between time series of photosynthesis and the final steady-state value[66].

Irradiance response curves. When A_n was at a steady state, i.e. before step changes in irradiance or at the end of a measurement sequence, 120 data points were used to extract average A_n at a given irradiance. The resulting values were used to construct steady-state irradiance response curves.

CO_2 response curves. Leaves were adapted to $1000\,\mu mol\ m^{-2}\ s^{-1}$ for ~30 min and 500 ppm C_a. C_a was then decreased stepwise until 50 ppm, each step taking 2–3 minutes. Thereafter, C_a was raised to 500 ppm, and after waiting for ~15 minutes, leaves were exposed to stepwise increases in C_a until 1500 ppm, each step taking ~4 minutes. Values were logged every 5 s and the last 60 s of every CO_2 step used to calculate average ± SEM of C_i and A_n. ϕ_{PSII} was determined at the end of each step as described above. Photosynthesis in all genotypes was corrected for CO_2 leaks using dried leaves of Col-0[54]. Parameters $V_{cmax,}$ J_{max}, and TPU were calculated after Sharkey *et al.*[55].

Statistical analysis. Each genotype was compared to Col-0 using a Student's *t*-test (Microsoft Excel, function t.test, assuming 2-tailed distribution and two-sample equal variance).

References

1. Pearcy, R. W., Roden, J. S. & Gamon, J. A. Sunfleck dynamics in relation to canopy structure in a soybean (Glycine max (L.) Merr.) canopy. *Agric. For. Meteorol.* **52,** 359–372 (1990).
2. Pearcy, R. W. Sunflecks and photosynthesis in plant canopies. *Annu. Rev. Plant Physiol.* **41,** 421–453 (1990).
3. Pearcy, R. W., Krall, J. P. & Sassenrath-Cole, G. F. Photosynthesis in fluctuating light environments. *Photosynth. Environ*. 321–346 (1996).
4. Kono, M. & Terashima, I. Long-term and short-term responses of the photosynthetic electron transport to fluctuating light. *J. Photochem. Photobiol. B Biol.* **137,** 89–99 (2014).
5. Kaiser, E. *et al.* Dynamic photosynthesis in different environmental conditions. *J. Exp. Bot.* **66,** 2415–2426 (2015).
6. Yamori, W. & Shikanai, T. Physiological Functions of Cyclic Electron Transport Around Photosystem I in Sustaining Photosynthesis and Plant Growth. *Annu. Rev. Plant Biol.* **67,** annurev-arplant-043015-112002 (2016).
7. Sassenrath-Cole, G. F. & Pearcy, R. W. The role of Ribulose-1,5-Bisphosphate regeneration in the induction requirement of photosynthetic CO_2 exchange under transient light conditions. *Plant Physiol.* **99,** 227–234 (1992).
8. Way, D. A. & Pearcy, R. W. Sunflecks in trees and forests: from photosynthetic physiology to global change biology. *Tree Physiol.* **32,** 1066–1081 (2012).
9. Küppers, M. & Pfiz, M. Role of photosynthetic induction for daily and annual carbon gains of leaves and plant canopies. *Photosynth. silico Underst. Complex. from Moelcules to Ecosyst*. 417–440 (2009).
10. Naumburg, E. & Ellsworth, D. S. Short-term light and leaf photosynthetic dynamics affect estimates of daily understory photosynthesis in four tree species. *Tree Physiol.* **22,** 393–401 (2002).
11. Murchie, E. H. & Niyogi, K. K. Manipulation of photoprotection to improve plant photosynthesis. *Plant Physiol.* **155,** 86–92 (2011).
12. Carmo-Silva, E., Scales, J. C., Madgwick, P. J. & Parry, M. A. J. Optimizing Rubisco and its regulation for greater resource use efficiency. *Plant. Cell Environ.* **38,** 1817–1832 (2015).
13. Seemann, J. R., Kirschbaum, M. U. F., Sharkey, T. D. & Pearcy, R. W. Regulation of Ribulose-1,5-Bisphosphate Carboxylase Activity in Alocasia macrorrhiza in Response to Step Changes in Irradiance. *Plant Physiol.* **88,** 148–152 (1988).
14. Stitt, M. & Grosse, H. Interactions between sucrose synthesis and CO_2 fixation I. Secondary kinetics during photosynthetic induction are related to a delayed activation of sucrose synthesis. *J. Plant Physiol.* **133,** 129–137 (1988).
15. Woodrow, I. E. & Mott, K. A. Rate limitation of non-steady-state photosynthesis by Ribulose-1,5-bisphosphate Carboxylase in spinach. *Aust. J. Plant Physiol.* **16,** 487–500 (1989).
16. Salvucci, M. E., Portis, A. R. J. & Ogren, W. L. A soluble chloroplast protein catalyzes ribulosebisphosphate carboxylase/oxygenase activation *in vivo*. *Photosynth. Res.* **7,** 193–201 (1985).
17. Salvucci, M. E., Werneke, J. M., Ogren, W. L. & Portis, A. R. Purification and species distribution of rubisco activase. *Plant Physiol.* **84,** 930–936 (1987).
18. Zhang, N. & Portis, A. R. Mechanism of light regulation of Rubisco: A specific role for the larger Rubisco activase isoform involving reductive activation by thioredoxin-f. *Proc. Natl. Acad. Sci. USA* **96,** 9438–9443 (1999).
19. Zhang, N., Kallis, R. P., Ewy, R. G. & Portis, A. R. Light modulation of Rubisco in Arabidopsis requires a capacity for redox regulation of the larger Rubisco activase isoform. *Proc. Natl. Acad. Sci. USA* **99,** 3330–3334 (2002).

20. Stitt, M., Lunn, J. & Usadel, B. Arabidopsis and primary photosynthetic metabolism - more than the icing on the cake. *Plant J.* **61,** 1067–1091 (2010).
21. Prinsley, R. T., Hunt, S., Smith, A. M. & Leegood, R. C. The influence of a decrease in irradiance on photosynthetic carbon assimilation in leaves of Spinacia oleracea L. *Planta* **167,** 414–420 (1986).
22. Zhu, X.-G., Ort, D. R., Whitmarsh, J. & Long, S. P. The slow reversibility of photosystem II thermal energy dissipation on transfer from high to low light may cause large losses in carbon gain by crop canopies: a theoretical analysis. *J. Exp. Bot.* **55,** 1167–1175 (2004).
23. Hubbart, S., Ajigboye, O. O., Horton, P. & Murchie, E. H. The photoprotective protein PsbS exerts control over CO_2 assimilation rate in fluctuating light in rice. *Plant J.* **71,** 402–412 (2012).
24. Armbruster, U. *et al.* Ion antiport accelerates photosynthetic acclimation in fluctuating light environments. *Nat. Commun.* doi: 10.1038/ncomms6439 (2014).
25. Vico, G., Manzoni, S., Palmroth, S. & Katul, G. Effects of stomatal delays on the economics of leaf gas exchange under intermittent light regimes. *New Phytol.* **192,** 640–652 (2011).
26. Allen, M. T. & Pearcy, R. W. Stomatal behavior and photosynthetic performance under dynamic light regimes in a seasonally dry tropical rain forest. *Oecologia* **122,** 470–478 (2000).
27. Alonso, J. M. *et al.* Genome-wide insertional mutagenesis of Arabidopsis thaliana. *Science*. **301,** 653–657 (2003).
28. Shan, X. *et al.* The role of Arabidopsis Rubisco activase in jasmonate-induced leaf senescence. *Plant Physiol.* **155,** 751–764 (2011).
29. Sun, J., Zhang, J., Larue, C. T. & Huber, S. C. Decrease in leaf sucrose synthesis leads to increased leaf starch turnover and decreased RuBP regeneration-limited photosynthesis but not Rubisco-limited photosynthesis in Arabidopsis null mutants of SPSA1. *Plant, Cell Environ.* **34,** 592–604 (2011).
30. Li, X.-P. *et al.* A pigment-binding protein essential for regulation of photosynthetic light harvesting. *Nature* **403,** 391–395 (2000).
31. Niyogi, K. K., Grossman, A. R. & Björkman, O. Arabidopsis mutants define a central role for the xanthophyll cycle in the regulation of photosynthetic energy conversion. *Plant Cell* **10,** 1121–1134 (1998).
32. Leon-Kloosterziel, K. *et al.* Isolation and characterisation of abscisic acid-deficient Arabidopsis mutants at two new loci. *Plant J.* **10,** 655–661 (1996).
33. Brosché, M. *et al.* Natural variation in ozone sensitivity among Arabidopsis thaliana accessions and its relation to stomatal conductance. *Plant, Cell Environ.* **33,** 914–925 (2010).
34. Veljovic-Jovanovic, S. D., Pignocchi, C., Noctor, G. & Foyer, C. H. Low Ascorbic Acid in the vtc-1 Mutant of Arabidopsis is Associated with Decreased Growth and Intracellular Redistribution of the Antioxidant System. *Plant Physiol.* **127,** 426–435 (2001).
35. Flexas, J. *et al.* Mesophyll conductance to CO_2 in Arabidopsis thaliana. *New Phytol.* **175,** 501–511 (2007).
36. Xing, H. T., Guo, P., Xia, X. L. & Yin, W. L. PdERECTA, a leucine-rich repeat receptor-like kinase of poplar, confers enhanced water use efficiency in Arabidopsis. *Planta* **234,** 229–241 (2011).
37. Bates, G. W. *et al.* A Comparative Study of the Arabidopsis thaliana Guard-Cell Transcriptome and Its Modulation by Sucrose. *Plos One* **7** (2012).
38. Farquhar, G. D. & Sharkey, T. D. Stomatal Conductance and Photosynthesis. *Annu. Rev. Plant Physiol.* **33,** 317–345 (1982).
39. Mate, C. J., Hudson, G. S., von Caemmerer, S., Evans, J. R. & Andrews, T. J. Reduction of Ribulose Bisphosphate Carboxylase Activase levels in tobacco (Nicotiana tabacum) by Antisense RNA reduces Ribulose Bisphosphate Carboxylase carbamylation and impairs photosynthesis. *Plant Physiol.* **102,** 1119–1128 (1993).
40. Mott, K. A. & Woodrow, I. E. Modelling the role of Rubisco activase in limiting non-steady-state photosynthesis. *J. Exp. Bot.* **51,** 399–406 (2000).
41. Yamori, W., Masumoto, C., Fukayama, H. & Makino, A. Rubisco activase is a key regulator of non-steady-state photosynthesis at any leaf temperature and, to a lesser extent, of steady-state photosynthesis at high temperature. *Plant J.* **71,** 871–880 (2012).
42. Carmo-Silva, A. E. & Salvucci, M. E. The regulatory properties of Rubisco activase differ among species and affect photosynthetic induction during light transitions. *Plant Physiol.* **161,** 1645–1655 (2013).
43. Brooks, A. & Portis, A. R. Protein-bound ribulose bisphosphate correlates with deactivation of ribulose bisphosphate carboxylase in leaves. *Plant Physiol.* **87,** 244–249 (1988).
44. Scales, J. C., Parry, M. A. J. & Salvucci, M. E. A non-radioactive method for measuring Rubisco activase activity in the presence of variable ATP: ADP ratios, including modifications for measuring the activity and activation state of Rubisco. *Photosynth. Res.* **119,** 355–365 (2014).
45. Lan, Y., Woodrow, I. E. & Mott, K. A. Light-dependent changes in ribulose bisphosphate carboxylase activase activity in leaves. *Plant Physiol.* **99,** 304–309 (1992).
46. Fay, P. A. & Knapp, A. K. Photosynthetic and stomatal responses of Avena sativa (Poaceae) to a variable light environment. *Am. J. Bot.* **80,** 1369–1373 (1993).
47. Tholen, D. *et al.* The chloroplast avoidance response decreases internal conductance to CO_2 diffusion in Arabidopsis thaliana leaves. *Plant, Cell Environ.* **31,** 1688–1700 (2008).
48. Flexas, J., Ribas-Carbó, M., Diaz-Espejo, A., Galmés, J. & Medrano, H. Mesophyll conductance to CO_2: current knowledge and future prospects. *Plant, Cell Environ.* **31,** 602–621 (2008).
49. Valladares, F., Allen, M. T. & Pearcy, R. W. Photosynthetic responses to dynamic light under field conditions in six tropical rainforest shrubs occuring along a light gradient. *Oecologia* **111,** 505–514 (1997).
50. McAusland, L., Davey, P. A., Kanwal, N., Baker, N. R. & Lawson, T. A novel system for spatial and temporal imaging of intrinsic plant water use efficiency. *J. Exp. Bot.* **64,** 4993–5007 (2013).
51. Li, X.-P., Muller-Moule, P., Gilmore, A. M. & Niyogi, K. K. PsbS-dependent enhancement of feedback de-excitation protects photosystem II from photoinhibition. *Proc. Natl. Acad. Sci. USA* **99,** 15222–15227 (2002).
52. Nilkens, M. *et al.* Identification of a slowly inducible zeaxanthin-dependent component of non-photochemical quenching of chlorophyll fluorescence generated under steady-state conditions in Arabidopsis. *Biochim. Biophys. Acta* **1797,** 466–475 (2010).
53. Huber, S. C., Nielsen, T. H., Huber, J. L. & Pharr, D. M. Variation among species in light activation of sucrose-phosphate synthase. *Plant Cell Physiol.* **30,** 277–285 (1989).
54. Long, S. P. & Bernacchi, C. J. Gas exchange measurements, what can they tell us about the underlying limitations to photosynthesis? Procedures and sources of error. *J. Exp. Bot.* **54,** 2393–2401 (2003).
55. Sharkey, T. D., Bernacchi, C. J., Farquhar, G. D. & Singsaas, E. L. Fitting photosynthetic carbon dioxide response curves for C3 leaves. *Plant, Cell Environ.* **30,** 1035–1040 (2007).
56. Sharkey, T. D. What gas exchange data can tell us about photosynthesis. *Plant, Cell Environ.* doi: 10.1111/pce.12641 (2015).
57. Scholl, R. L., May, S. T. & Ware, D. H. Seed and molecular resources for Arabidopsis. *Plant Physiol.* **124,** 1477–1480 (2000).
58. van Rooijen, R., Aarts, M. G. M. & Harbinson, J. Natural genetic variation for acclimation of photosynthetic light use efficiency to growth irradiance in Arabidopsis thaliana. *Plant Physiol.* **167,** pp.114.252239 (2015).
59. Gibeaut, D. M., Hulett, J., Cramer, G. R. & Seemann, J. R. Maximal biomass of Arabidopsis thaliana using a simple, low-maintenance hydroponic method and favorable environmental conditions. *Plant Physiol.* **115,** 317–319 (1997).
60. Yin, X., Sun, Z., Struik, P. C. & Gu, J. Evaluating a new method to estimate the rate of leaf respiration in the light by analysis of combined gas exchange and chlorophyll fluorescence measurements. *J. Exp. Bot.* **62,** 3489–3499 (2011).
61. Walker, B., Ariza, L. S., Kaines, S., Badger, M. B. & Cousins, A. B. Temperature response of *in vivo* Rubisco kinetics and mesophyll conductance in Arabidopsis thaliana: comparisons to Nicotiana tabacum. *Plant. Cell Environ.* **36,** 2108–2119 (2013).

62. Cleveland, W. S., Grosse, E. & Shyu, W. M. In *Stat. Model. S* (Chambers, J. M. & Hastie, T. J.) (Wadsworth & Brooks/Cole, 1992).
63. Allen, M. T. & Pearcy, R. W. Stomatal versus biochemical limitations to dynamic photosynthetic performance in four tropical rainforest shrub species. *Oecologia* **122,** 479–486 (2000).
64. Pons, T. L., Pearcy, R. W. & Seemann, J. R. Photosynthesis in flashing light in soybean leaves grown in different conditions. I. Photosynthetic induction state and regulation of ribulose-1,5-bisphosphate carboxylase activity. *Plant, Cell Environ*. **15,** 569–576 (1992).
65. Vines, H. M., Tu, Z.-P., Armitage, A. M., Chen, S.-S. & Black, C. C. J. Environmental responses of the post-lower illumination CO_2 burst as related to leaf photorespiration. *Plant Physiol*. **73,** 25–30 (1983).
66. Tomimatsu, H. *et al.* High CO_2 concentration increases relative leaf carbon gain under dynamic light in Dipterocarpus sublamellatus seedlings in a tropical rain forest, Malaysia. *Tree Physiol*. **34,** 944–954 (2014).

Acknowledgements

We thank the Nottingham Arabidopsis Stock Centre, Corrie Hanhart, Elizabete Carmo-Silva and Shizue Matsubara for providing *A. thaliana* seeds. Also, we thank Sasan Aliniaeifard for help with the growth system. We thank Shizue Matsubara and Tom Sharkey for helpful discussions. This work was carried out within the BioSolar Cells programme. It was funded by the Dutch Ministry of Economic Affairs and Powerhouse.

Author Contributions

Design of experiment: all authors. Execution of experiment: E.K. and A.M. Data analysis and interpretation: A.M. and E.K. Writing of manuscript: all authors.

Additional Information

Supplementary information accompanies this paper at http://www.nature.com/srep

Competing financial interests: The authors declare no competing financial interests.

How to cite this article: Kaiser, E. *et al.* Metabolic and diffusional limitations of photosynthesis in fluctuating irradiance in *Arabidopsis thaliana*. *Sci. Rep.* **6**, 31252; doi: 10.1038/srep31252 (2016).